

SYNTHESIS OF  $\text{La}_x\text{Sr}_{1-x}\text{TiO}_3$  ANODE MATERIALS BY SOL-GEL AUTO-COMBUSTION METHODJIHAI CHENG<sup>1\*</sup>

Department of Chemistry and Materials Engineering, Hefei University, Hefei, 230022, China  
(Received: December 3, 2010 - Accepted: October 7, 2011)

## ABSTRACT

A novel anode material for intermediate temperature solid oxide fuel cells with a composite of  $\text{La}_x\text{Sr}_{1-x}\text{TiO}_3$  has been synthesized by a sol-gel auto-combustion method. X-ray diffraction (XRD) shows that  $\text{La}_x\text{Sr}_{1-x}\text{TiO}_3$  has good chemical compatibility with  $\text{Gd}_{0.2}\text{Ce}_{0.8}\text{O}_{1.9}$  electrolyte. The thermal expansion coefficient (TEC) of the as-prepared anode material is similar to that of  $\text{Gd}_{0.2}\text{Ce}_{0.8}\text{O}_{1.9}$ . The electric conductivity measurements show that the conductivity of  $\text{La}_x\text{Sr}_{1-x}\text{TiO}_3$  increases with the increasing of lanthanum contents and reached a maximal value at  $x=0.3$ . At 800°C, the electrical conductivity of  $\text{La}_{0.3}\text{Sr}_{0.7}\text{TiO}_3$  is  $184\ \text{S}\cdot\text{cm}^{-1}$ .

**Keywords:** Fuel cells; Electrode materials; Chemical synthesis; X-ray diffraction

## 1. INTRODUCTION

Solid oxide fuel cells (SOFCs) are currently regarded as one of new energy conversion systems because of their high efficiency, environmentally friendly technology and fuel flexibility [1]. However, SOFCs still have many problems related to its longevity or long term stability due to its high operation temperature, and the majority of current researches is concentrated on the development of intermediate temperature SOFCs (IT-SOFCs) [2,3]. Recently, there are intensive studies on the anode of solid oxide fuel cells, and Ni-cermet composites are the most commonly used materials as anodes for IT-SOFCs [4-6]. Traditional Ni-yttria stabilized zirconia (Ni/YSZ) anodes have been used in SOFCs for decades. Although nickel is an excellent catalyst for hydrogen oxidation and good electrical current conductor, Ni-based anodes are likely to suffer structural damage when cycled repeatedly in oxidizing and reducing atmospheres [7-10]. Therefore, research and development of new anode materials have received much attention previously.

Perovskite-type oxide materials have attracted many attentions as IT-SOFCs anodes due to their mixed-conducting characteristics and higher ionic conductivity in the intermediate temperature range [11-13]. Among those perovskite-type oxides,  $\text{SrTiO}_3$  shows great potential as an anode material and receives considerable attentions.  $\text{SrTiO}_3$  shows ionic conduction, mixed ionic-electronic conduction or electronic conduction by the use of dopants, and the electrical behaviour of such material may be adjusted by the proper choice of the donor dopant [14, 15]. It has been reported that doped  $\text{SrTiO}_3$  possesses good electrical and thermal properties as the anode in SOFCs, and they have been found to be dimensionally stable during oxidation-reduction cycling [16, 17]. So they are employed as the candidate anode materials for IT-SOFCs.

This study is part of a more general goal to develop new anode materials and designs, which solve the problems associated with the current Ni/YSZ cermet anode. Perovskite-type composite oxides with a general formula  $\text{La}_x\text{Sr}_{1-x}\text{TiO}_3$  ( $x=0.1-0.4$ ) (LST) were prepared by a sol-gel auto-combustion process. In order to elucidate the performances, the electrical conductivity and chemistry compatibility with gadolinium-doped ceria ( $\text{Gd}_{0.2}\text{Ce}_{0.8}\text{O}_{1.9}$ , GDC) electrolyte of this material were measured.

## 2. EXPERIMENTAL

The new anode materials with a general formula  $\text{La}_x\text{Sr}_{1-x}\text{TiO}_3$  ( $x=0.1-0.4$ ) were prepared by a sol-gel auto-combustion process. Powder samples with the general formula of  $\text{La}_x\text{Sr}_{1-x}\text{TiO}_3$  (LST) were synthesized by the sol-gel auto-combustion process, as shown in Fig.1.

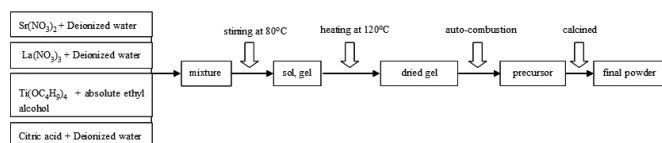


**Fig.1.** Flow chart of preparing  $\text{La}_x\text{Sr}_{1-x}\text{TiO}_3$  powder by the sol-gel auto-combustion process.

The starting substances are aqueous solutions of analytically pure grade  $\text{Sr}(\text{NO}_3)_2$ ,  $\text{La}(\text{NO}_3)_3$ ,  $\text{Ti}(\text{OC}_4\text{H}_9)_4$  and citric acid (China National Medicines Corporation Ltd., China). This forms a sol, gel by heating at about 80°C and wet gel was further heated to about 120°C to remove the solvents. The dried gel was baked in an oven at 500-700°C where the combustion reaction took place to form the precursors. The powders were prepared by calcining the precursors at 700-900°C for 3h. The powders were characterized by an X-ray diffractometer (XRD) (D/max-γB, Rigaku, Japan). The thermal expansion coefficient was tested using a Dilatometer in an air atmosphere at an increase rate of  $10^\circ\text{C}\cdot\text{min}^{-1}$ . The electrical conductivity of rectangular bar specimens ( $35\text{mm}\times 5\text{mm}\times 1.8\text{mm}$ ) calcined at 1300°C was tested from 500 to 800°C in hydrogen atmosphere using standard DC four-probe technique.

## 3. RESULTS AND DISCUSSION

## 3.1. Crystalline phases

Fig.2 shows the XRD patterns of  $\text{La}_{0.3}\text{Sr}_{0.7}\text{TiO}_3$  samples calcined at different temperatures. Although the typical diffraction peaks of perovskite structure occur at 700°C, but there still have many other diffraction peaks, which indicate that the sample was not well crystallized at this temperature (shown in Fig. 2a). When the sintering temperature increases to 800°C, the appearance of the 110, 200, 111 and 211 typical diffraction peaks indicate that the  $\text{La}_{0.3}\text{Sr}_{0.7}\text{TiO}_3$  powders have crystallized and formed cubic perovskite structure. However, there still appear few obscure diffraction peaks, especially at  $2\theta=25^\circ-27^\circ$ ,  $2\theta=37^\circ$  and  $2\theta=44.5^\circ$  (shown in Fig. 2b). After calcined at 900°C for 3h, these phases were well crystallized and no second phases are identified (shown in Fig. 2c), implying that the resultant  $\text{La}_{0.3}\text{Sr}_{0.7}\text{TiO}_3$  powders appear crystalline as a good-cubic perovskite structure similar to the standard pattern of  $\text{SrTiO}_3$  (JCPDS No.35-0734).

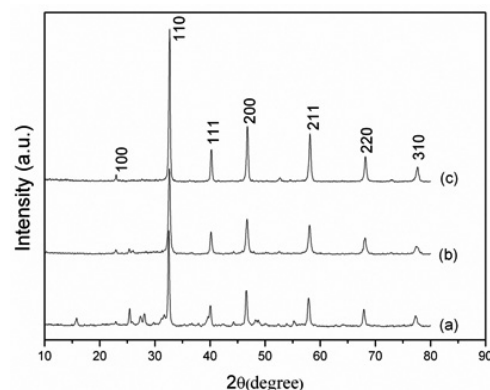


**Fig.2.** X-ray diffraction patterns of  $\text{La}_{0.3}\text{Sr}_{0.7}\text{TiO}_3$  powders calcined at (a) 700°C; (b) 800°C; (c) 900°C.

### 3.2. Thermal-expansion behavior

The thermal expansion measurements for LST were carried out in the temperature range of 50-800°C. The thermal expansion curve of  $\text{La}_{0.3}\text{Sr}_{0.7}\text{TiO}_3$  sample after sintering at 1300°C for 5h is shown in Fig.3.

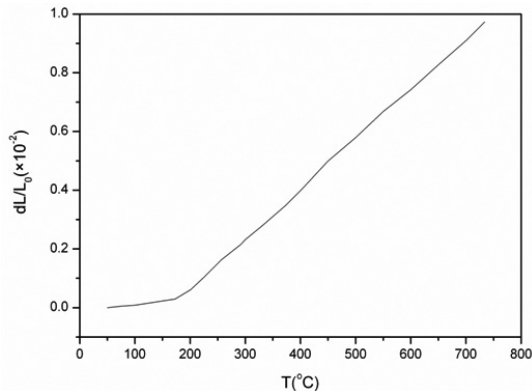


Fig.3. Dilatometric curves of  $\text{La}_{0.3}\text{Sr}_{0.7}\text{TiO}_3$  sample in air.

It shows linear dependences with the testing temperature. In the range of 50-750°C, the average thermal expansion coefficients(TEC) value of LST is  $11.74 \times 10^{-6} \text{K}^{-1}$  which is very close to that of GDC electrolyte ( $12 \times 10^{-6} \text{K}^{-1}$ ) [18]. From the viewpoint of thermal expansion, the new LST anode material has good physical compatibility with GDC and has a matching TEC with the GDC electrolyte.

### 3.3. Electrical conductivity

When the samples were sintered under reducing atmosphere, the oxygen volatilization is easy to occur, and formed the oxygen vacancy. Doped  $\text{SrTiO}_3$  have the electronic-ion mix conduction characteristic under the reducing atmosphere. Fig. 4 shows the temperature dependence of the conductivity of  $\text{La}_x\text{Sr}_{1-x}\text{TiO}_3$  samples prepared by sintering at 1300°C for 5h.

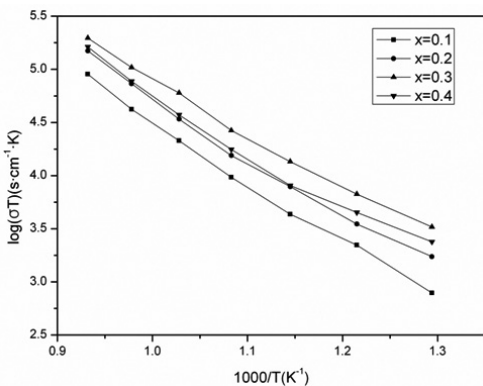


Fig.4. Temperature dependence of the conductivity of  $\text{La}_x\text{Sr}_{1-x}\text{TiO}_3$  samples under hydrogen atmosphere.

Results show that the electrical conductivity of  $\text{La}_x\text{Sr}_{1-x}\text{TiO}_3$  increase with the increasing of lanthanum contents and reach a maximal value at  $x=0.3$ . At 800°C, the conductivities of  $\text{La}_{0.1}\text{Sr}_{0.9}\text{TiO}_3$ ,  $\text{La}_{0.2}\text{Sr}_{0.8}\text{TiO}_3$ ,  $\text{La}_{0.3}\text{Sr}_{0.7}\text{TiO}_3$  and  $\text{La}_{0.4}\text{Sr}_{0.6}\text{TiO}_3$  are  $84 \text{S} \cdot \text{cm}^{-1}$ ,  $139 \text{S} \cdot \text{cm}^{-1}$ ,  $184 \text{S} \cdot \text{cm}^{-1}$  and  $152 \text{S} \cdot \text{cm}^{-1}$ , respectively. On one hand, after partial substitution of  $\text{Sr}^{2+}$  with  $\text{La}^{3+}$ , the oxygen vacancy concentration in  $\text{La}_x\text{Sr}_{1-x}\text{TiO}_3$  increased with the increasing of  $\text{La}^{3+}$  content, composition of ionic conductor in the sample increases, then the conductivity increases gradually in the range of  $x=0.1-0.3$ . But when the amount of the substituted  $\text{La}^{3+}$  ions exceeded a certain value ( $x=0.4$ ), the density of the sample will be decrease, thus the conductivity decrease. On the other hand, for the doped  $\text{La}_x\text{Sr}_{1-x}\text{TiO}_3$ , the substitution of La for Sr resulted in an excess electron due to the different valence state of  $\text{La}^{3+}$  and  $\text{Sr}^{2+}$ , and  $\text{La}_x\text{Sr}_{1-x}\text{TiO}_3$  are n-type conductors because this electron was excited, thus leading to the increase of electrical conductivity with La content in LST [19,20]. However, the

compounds with  $x \geq 0.4$  are p-type semiconductors, in the case of such p-type conductors, the conductivity decreases because of the decrease of charge carriers in combination with an increase of oxygen vacancies [21]. Therefore,  $\text{La}_x\text{Sr}_{1-x}\text{TiO}_3$  possessed relatively high electrical conductivity at a proper La content, this may be an attractive property for the use of  $\text{La}_x\text{Sr}_{1-x}\text{TiO}_3$  for an anode in SOFCs.

### 3.4. Chemical stability

In order to examine the chemical compatibility of  $\text{La}_x\text{Sr}_{1-x}\text{TiO}_3$  and GDC, chemical compatibility experiment was carried out with the mixed powders of  $\text{La}_{0.3}\text{Sr}_{0.7}\text{TiO}_3$  and GDC in a weight ratio of 1:1. The GDC powders were prepared by the combustion method [22].

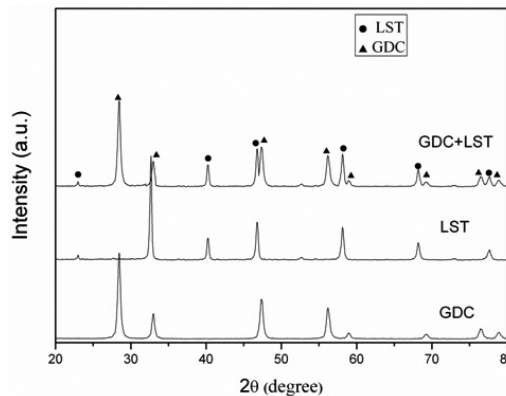


Fig.5. XRD patterns of LST, GDC and LST/GDC composite sintered 1300°C.

Fig. 5 shows XRD patterns of LST, GDC and the binary-mixed system of LST-GDC heated at 1300°C for 5h, respectively. The XRD analysis shows that the XRD pattern of the prepared LST powder matches well with the diffraction data for perovskite phase. The results for GDC show the single standard cubic fluorite structure. No additional diffraction peaks other than the peaks for pure LST and GDC phases were found in the LST -GDC system, the XRD patterns still showed two phases: perovskite phase of LST and cubic fluorite structure of GDC, indicating that no interfacial reaction between the  $\text{La}_x\text{Sr}_{1-x}\text{TiO}_3$  anode material and GDC electrolyte. Therefore, there has the long-term stability of LST-GDC and no significant reaction layer could be found at the LST/GDC interface after long-term operation test at intermediate temperature range.

## 4. CONCLUSIONS

A novel anode material has been synthesized using a sol-gel auto-combustion process with a general formula of  $\text{La}_x\text{Sr}_{1-x}\text{TiO}_3$ . It shows a unique structure with the fine cubic perovskite structure when the precursors calcined at 900°C. LST anode material has a matching TEC with GDC electrolyte as well as showing linear thermal expansion behavior in air, and it has the long-term stability with the GDC electrolyte. The electric conductivity measurements show that the conductivity of LST increase with the increasing of lanthanum contents and reached a maximal value at  $x=0.3$ . At 800°C, the conductivities of  $\text{La}_{0.3}\text{Sr}_{0.7}\text{TiO}_3$  is  $184 \text{S} \cdot \text{cm}^{-1}$ .

## REFERENCES

- [1] N.Q. Minh, J Am Ceram Soc. 76, 563, (1993)
- [2] Y. Ji, Y.H. Huang, J.R. Ying, J.B. Goodenough, Electrochem. Commun. 9, 1881, (2007)
- [3] H. Zhao, D. Teng, X. Zhang, C. Zhang, X. Li, J Power Sources. 186, 305, (2009)
- [4] N.Q. Minh, Solid State Ionics. 174, 271, (2004)
- [5] C. Sun, U. Stimming, J Power Sources. 171, 247, (2007)
- [6] J.H. Wang, M. Liu, Electrochem Commun. 9, 2212, (2007)
- [7] X. Sun, S. Wang, Z. Wang, J. Qian, T. Wen, F. Huang, J Power Sources. 187, 85, (2009)
- [8] Q.X. Fu, F. Tietz, D. Stover, J Electrochem Soc. 153, 74, (2006)
- [9] M. Gong, X. Liu, J. Tremblay, C. Johnson, J Power Sources. 168, 289, (2007)

- [10] J.B. Goodenough, Y.H. Huang, *J Power Sources*. 173, 1, (2007)
- [11] Z. Lei, Q. Zhu, L. Zhao, *J Power Sources*. 161, 1169, (2006)
- [12] S.P. Jiang, W.Wang, *Solid State Ionics*. 176, 1351, (2005)
- [13] X.D. Zhu, K.N. Sun, N.Q. Zhang, X.B. Chen, L.J.Wu, D.C. Jia, *Electrochem Commun*. 9, 431, (2007)
- [14] S.Hashimoto, L.Kindermann, F.W.Poulsen, M.Mogensen, *J Alloys Compd*. 397, 245, (2005)
- [15] H. Lu, J. Tong, Z. Deng, Y. Cong, W. Yang, *Materials Res Bull*. 41, 683, (2006)
- [16] O.A. Marina, N.L. Canfield, J.W. Stevenson, *Solid State Ionics*. 149, 21, (2002)
- [17] H. Kurokawa, L. Yang, C.P. Jacobson, L.C. De Jonghe, S.J. Visco, *J Power Sources*. 164, 510, (2007)
- [18] H. Hayashi, M. Kanoh, C.J. Quan, H. Inaba, S.R. Wang, M. Dokiya, H. Tagawa, *Solid State Ionics*. 132, 227, (2000)
- [19] V. Vashook, L. Vasylechko, J. Zosel, U. Guth, *Solid State Ionics*. 159, 279, (2003)
- [20] P.D. Battle, J.E. Brnnett, J. Sloan, R.J.D. Tilley, J.F. Vente, *J. Solid State Chemistry*. 149, 360, (2000)
- [21] I. Yasuda, M. Hishinuma, *Solid State Ionics*. 80, 141, (1995)
- [22] T. Mahata, G. Das, R.K. Mishra, B.P. Sharma, *J Alloys Compd*. 391, 129, (2005).